Technical note: Long-term memory loss of urban streams as a metric for catchment classification

Dusan Jovanovic[1], Tijana Jovanovic[2], Alfonso Mejía[2], Jon Hathaway[3], Edoardo Daly[1]

[1]Department of Civil Engineering, Monash University, Melbourne, 3800, VIC, Australia
5 [2]Department of Civil and Environmental Engineering, The Pennsylvania State University, University Park, 16802, PA, USA
[3]Department of Civil and Environmental Engineering, The University of Tennessee, Knoxville, 37996, TN, USA

Correspondence to: Edoardo Daly (edoardo.daly@monash.edu)

10   **Abstract.**

Urbanisation has been associated with a reduction in the long-term correlation within a streamflow series, quantified by the Hurst exponent (H). This presents an opportunity to use the H exponent as an index for the classification of catchments on a scale from natural to urbanised conditions. However, before using the H exponent as a general index, the relationship between this exponent and level of urbanisation needs to be further examined
15   and verified on catchments with different levels of imperviousness and from different climatic regions. In this study, the H exponent is estimated for 38 (deseasonalized) mean daily runoff time series, 22 from the USA and 16 from Australia, using the traditional rescaled-range statistic (R/S) and the more advanced multi-fractal detrended fluctuation analysis (MF-DFA). Relationships between H and catchment imperviousness, catchment size, annual rainfall and specific mean discharge were investigated. No clear relationship with catchment area was
20   found, and a weak negative relationship with annual rainfall and specific mean streamflow was found only when the R/S method was used. Conversely, both methods showed decreasing values of H as catchment imperviousness increased. The H exponent decreased from around 1.0 for catchments in natural conditions to around 0.6 for highly urbanised catchments. Three significantly different ranges of H exponents were identified, allowing catchments to be parsed into groups with imperviousness lower than 5% (natural), catchments with imperviousness between
25   5 and 15 % (peri-urban), and catchments with imperviousness larger than 15% (urban). The H exponent thus represents a useful metric to quantitatively assess the impact of catchment imperviousness on streamflow regime.

1 Introduction

The increase in the degree of urbanization of a catchment is known to adversely influence streamflow quantity and quality (Paul and Meyer, 2001). Larger peak-flows and reduced times to peak are well known characteristics
30   of urban streams (Leopold, 1968), while lower baseflow rates are often but not always observed (Hamel et al., 2015). At the same time, the larger flows discharged in urban streams increase the export of nutrients and pollutants, and cause a decrease in biodiversity with associated detrimental effects to the health of riparian ecosystems (Walsh et al., 2005b). Although traditionally focused on peak flows, the management of urban stormwater runoff is now often directed toward restoration of the overall streamflow regime, which includes the
35   dynamic range of streamflow fluctuations (see Mejía et al., 2014). Therefore, the management of urban streams has been increasingly focused on controlling urban stormwater runoff with the intent to limit the streamflow during floods while also maintaining adequate flow rates during dry periods (Debusk et al., 2011; Burns et al.,

2012). This management strategy is often linked to the natural flow paradigm (Poff, 1997), which advocates the maintenance of streams as close as possible to their natural regime.

Accordingly, streams affected by urbanization should be managed to achieve streamflow regimes similar to predevelopment conditions. It is thus important to quantify the effect of urbanization on streamflow and

5   systematically classify urban catchments according to their level of development (e.g., McDonnell and Woods, 2004; Wagener et al., 2007; Sivakumar and Singh, 2012). A number of indexes are available for assessing the changes in hydrological regimes of rivers and streams (Olden and Poff, 2003; Poff et al., 2010); however, only a subgroup has been tested for application to a specific flow component (baseflow) in urbanized catchments (Hamel et al., 2015). These indexes are often grouped depending on the information they give about certain flow

10   characteristics, such as magnitude, frequency, and duration. The selection of appropriate metrics that are applicable to different locations and climatic conditions is still an unresolved issue, with statistical methods often employed to avoid the use of metrics which provide redundant information on the streamflow regime (e.g., Olden and Poff, 2003; Poff et al., 2010; Hamel et al., 2015). Despite these efforts, it is still difficult to define a single streamflow metric that can summarize where a catchment lies across the spectrum of conditions from natural to

15   fully urbanized.

Because urbanization facilitates the rapid delivery of precipitation to streams due to impervious areas and the direct connection between land and stream via drainage systems (Hamel et al., 2013; Epps and Hathaway, *in press*), the resulting flashier hydrographs and the lower baseflow rates in urban areas have been associated with a possible reduction in long-term correlation (Jovanovic et al., 2016; Kim et al., 2016). A measure of long-term

20   correlation is represented by the Hurst exponent (e.g., Beran, 1994), which has been largely used to characterized streamflow time series (Hurst, 1951; Mandelbrot and Wallis, 1969; Montanari et al., 1997; Koutsoyiannis, 2002; Szolgayova et al., 2014; Jovanovic et al., 2016; Ausloos et al., 2017). The Hurst exponent equals 0.5 for an uncorrelated white noise signal, while values larger than 0.5, as commonly found for streamflow series, are associated with persistent processes (e.g., Serinaldi, 2010). Because urbanization, with the quicker delivery of

25   stormwater runoff to streams, is likely to break the long-term correlation often found in rural and natural streams, one would expect the Hurst exponent of urban streams to be closer to 0.5 when compared to rural and natural streams. Following this hypothesis, Jovanovic et al. (2016) and Kim et al. (2016) reported a decrease in values of the Hurst exponent with an increase in catchment imperviousness. Thus, although not listed in the large number of metrics often used to classify streams, the Hurst exponent has the potential to quantify the impact of

30   urbanization on stream hydrology. However, there is a need to further examine the relationship between the Hurst exponent and the level of urbanization of a catchment by 1) including more catchments into the analysis in order to better estimate the relationship, and 2) include catchments from different geographic and climatic regions to explore whether the observed relationship is site-independent.

The aim of this study is to investigate the utility of the Hurst exponent to estimate the impacts of urbanization on

35   stream hydrology, thereby providing a general index for the classification of different levels of catchment urbanization.

2 Methods

2.1 Estimation of long-term dependence within a streamflow time series

Two methods were applied to estimate the Hurst exponent, H. The first method is the oldest and well-known rescaled range statistics (R/S) (Hurst, 1951) as proposed by Mandelbrot and Wallis (1969). Although this method

5   has limitations compared to other more sophisticated estimations of scaling indexes (Montanari et al., 1997; Szolgayova et al., 2014), it is rather simple and thus popular to detect long-term memory by way of estimating H. The second method is multifractal detrended fluctuation analysis (MF-DFA) (Kantelhardt et al., 2002).

For both methods, the analysis starts by creating from the original series of length L the fluctuation series, ϕ_j ($j = 1, .., L$), which does not have seasonal cycles. Seasonal cycles are removed from the original series by subtracting

10   the calendar day mean and dividing by the calendar day standard deviation (Kantelhardt et al., 2002; Szolgayova et al., 2014). The R/S and the MF-DFA are then applied to the series ϕ_j.

The details of the R/S method can be found in Weron (2002) and Szolgayova et al. (2014). The time series ϕ_j is divided into D subseries of length N. For each of the m subseries ($m = 1, ..., D$), the following calculations are performed:

15   1)   The mean E_m and standard deviation S_m of the subseries are calculated.

     2)   The subseries, $\phi_{i,m}$, is normalized by subtracting the sample mean to obtain (Equation 1):

$$X_{i,m} = \phi_{i,m} - E_m$$

(1)

20

     for $i = 1, ..., N$.

     3)   Cumulative time series are created as (Equation 2):

$$Y_{i,m} = \sum_{j=1}^{i} X_{j,m}$$

25   (2)

     for $i = 1, ..., N$.

     4)   The range is calculated as (Equation 3):

30      $$R_m = \max\{Y_{1,m}, ..., Y_{n,m}\} - \min\{Y_{1,m}, ..., Y_{n,m}\}$$

(3)

     and then rescaled as R_m/S_m.

Once these steps have been repeated for the m subseries with length N, the mean value of the rescaled range for

35   all subseries of length N is calculated as (Equation 4):

$$(R/S)_N = \frac{1}{D}\sum_{m=1}^{D} R_m/S_m.$$

(4)

These operations are performed for different values of N. The minimum length of the subseries used in this study was 10 days, while the maximum length was ¼ of the total length of the available time series. Since the R/S statistics asymptotically follows the relationship $(R/S)_N \sim cN^H$ (Mandelbrot and Wallis, 1969), the value of H is estimated as the slope of the linear least squares regression (Equation 5):

$$\log(R/S)_N = \log c + H \log N.$$
(5)

The details of the MF-DFA method can be found in, e.g., Jovanovic et al. (2016). The following calculations are performed on the time series ϕ_j:

1) The so-called profile value at i of the fluctuation series is created as (Equation 6):

$$W(i) = \sum_{k=1}^{i} \phi_k.$$
(6)

The profile is segmented into non-overlapping intervals of duration s (Equation 7):

$$N_s = int(N/s)$$
(7)

2) Local trends from each N_s segment are removed by fitting a polynomial trend to each segment and removing it from the series. This permits the calculation of the fluctuation function for each segment as (Equation 8):

$$F^2(v,s) = \frac{1}{s}\sum_{i=1}^{s}[W(vs+i) - p_{n,v}(i)]^2,$$
(8)

where v indexes the different segments $v = 0, \ldots, N_s - 1$ and $p_{n,v}(i)$ is the value at i of the polynomial fit of order n in segment v.

3) Since the record length N is unlikely a multiple of s, to avoid disregarding that portion of the record, the fluctuation function is also computed starting from the end of the record as (Equation 9):

$$F^2(v,s) = \frac{1}{s}\sum_{i=1}^{s}[W(N - (v - N_s + 1)s + i) - p_{n,v}(i)]^2.$$
(9)

To find the overall q^{th} order fluctuation for the timescale s, the fluctuations from each segment are averaged such that

$$F_q(s) = \left\{ \frac{1}{2N_s} \sum_{i=0}^{2N_s-1} [F^2(v,s)]^{q/2} \right\}^{1/q}.$$

10)

5 When the time series has a long-term power-law correlation, one expects that $F_q(s) \sim s^{h(q)}$, where $h(q)$ is the generalized Hurst exponent (Kantelhardt et al., 2002). In the case q =1, $h(1)$ corresponds to the Hurst exponent from the R/S analysis (Kantelhardt et al., 2006). To obtain the scaling exponent $h(q)$, $F_q(s)$ is plotted as a function of s in log-log space and a line is fitted to the data using the least square regression. In this study, q was 1 and the order of the polynomial fitting function was 5.

10 The values of H obtained for different streamflow series were then grouped according to the level of impervious cover (i.e. level of urbanization of catchments) to select natural, peri-urban, and urban catchments. A two sample t-test and Wilcoxon rank-sum test was applied to test the difference between the empirical distributions of the Hurst exponents for these three different groups of catchments.

2.2 Data

15 Thirty eight time series of mean daily streamflows were used for this study, as detailed in Table 1. Twenty two streamflow gauging stations were located in the USA and sixteen were in Australia. The US stations were located in the metropolitan areas of the cities of Baltimore, Philadelphia and Washington, DC, and the Australian stations were located in the metropolitan area of the city of Melbourne. The locations of these monitoring stations within the USA and Australia were visualized on maps in Jovanovic et al. (2016) and Hamel et al. (2015), respectively.

20 The mean annual rainfall for US catchments ranged from around 1000 mm to 1250 mm. The mean annual rainfall for the Australian catchments located close to the city is about 700 mm (Melbourne water station 229636A for the period 1978-2016), while some of the outlaying catchments having low to no imperviousness receive up to about 1100 mm (Melbourne water station 229111A for the period 1990-2016). The air temperature range for US catchments is from -20 to 41 °C with an average of 13 °C, while the air temperature for Australian catchments

25 ranges from -3 to 47 °C with an average of 15 °C. The level of catchment urbanization for each of the stations was indicated by the fraction of total impervious cover (i.e. imperviousness, U [%]), which ranged from zero (i.e. natural conditions) to nearly 50 % (i.e. largely urbanized catchments).

3 Results and Discussion

30 The values of H obtained using R/S analysis were between about 0.6 to around 0.9, while the MF-DFA analysis resulted in slightly higher values, ranging from 0.65 to around 1.1 (Figure 1); MF-DFA can give estimates slightly higher than 1 (Serinaldi, 2010), suggesting that the process is persistent (Li and Zhang, 2007).

Regardless of the method used, the obtained values of H showed a decreasing trend with the increase in imperviousness for both US and Australian catchments (Spearman correlation coefficient ρ = -0.68, p<0.001 for

35 R/S method and ρ = -0.77, p<0.001 for MF-DFA method; Figure 1). The decreasing trend appears to stop around 15% imperviousness; increasing the impervious fraction beyond 15% does not seem to be associated with a further decrease of the estimated values of H. From Figure 1, it appears that the rapid release of stormwater runoff to

urban streams, which generates the well-known flashiness in urban streamflow series (e.g. Leopold, 1968; Paul and Meyer, 2001) breaks the long-term correlation within the time series, as reflected by the lower values of H. Conversely, the catchments in natural conditions have the highest values of H due the high precipitation filtering capacity of natural landscapes.

5 This decrease in the long-term dependence of the streamflow time series has been observed in previous studies (Jovanovic et al., 2016; Kim et al., 2016). Jovanovic et al. (2016), using data from the same US catchments as the present study, showed that the temporal structure of the streamflow for the most urbanized US catchments was similar to the temporal structure of the precipitation records. This suggests that the increase in impervious cover might cause more precipitation to bypass the groundwater storage, a logical outcome given the known influences of imperviousness on infiltration potential. Furthermore, the urban stormwater network tends to enhance the delivery of water from directly connected areas to urban streams. Although direct connectivity was not explicitly considered in this study, one would expect impervious fraction and direct connectivity to be highly correlated. The elevated degree of direct connectivity in highly impervious catchments may have contributed to the decrease in the H exponent. Because new developments in both USA and Australia are increasingly implementing stormwater green infrastructure that reduces connectivity between impervious areas and urban streams, it is possible that the reduction of H will become less visible in the future.

The obtained values of H can be parsed into three groups according to their impervious cover fraction (Figure 1). Catchments with less than 5% impervious areas have larger values of H ($0.75<H<1$ using R/S and $0.9<H<1.2$ using MF-DFA), while those with values of imperviousness larger than 15% are mostly related to lower values of H ($0.6<H<0.75$ using R/S and $0.6<H<0.9$ using MF-DFA). This is consistent with experimental observations, which showed that imperviousness as low as 15-20% is sufficient to impact stream health and ecology (e.g., Arnold and Gibbons, 1996; Walsh et al., 2005a). Between 5% and 15% the values of H appear more scattered. Therefore, the three levels of imperviousness defined from Figure 1 can be classified as natural ($U\leq5\%$), peri-urban ($5\%<U\leq15\%$), and urban ($U>15\%$) catchments based on the corresponding range of values of H. Similar classification ranges were reported in the literature previously (e.g., Hamel et al., 2015), although they were not based on a metric easily quantifiable from streamflow series. The relationship between H and catchment imperviousness appears to be more evident for the US catchments, as the Australian streamflow series for two highly urbanized catchments (i.e., Blind Creek @ Knox and Gardiners Creek @ Kinkora) resulted in values of H comparable to peri-urban catchments, potentially due to data gaps. Nevertheless, when considered together as three different groups (i.e., natural, peri-urban and urban), the empirical distributions of H corresponding to these groups are significantly different from each other ($p<0.05$, t-test and $p<0.05$, Wilcoxon rank-sum test) for both the R/S and MF-DFA methods (Figure 2).

Because other variables and catchment attributes can affect the value of H, the estimated H exponents were also related to the catchment area and catchment wetness.

Previous studies identified a positive relationship between H and catchment area (e.g., Mudelsee, 2007; Hirpa et al., 2010; Szolgayova et al., 2014). The increase in long-term dependence has been hypothesized as being due to the increase in storage capacity (e.g., groundwater, inundations) with increasing catchment size. However, no relationship was found between these two variables for the dataset in Table 1, as shown in Figure 3 ($\rho = 0.24$, p =

0.15 for R/S method and $\rho = 0.28$, $p = 0.09$ for MF-DFA method). These conflicting results may be due to the smaller size of urban catchments compared to those in literature. For example, the size of the largest catchment used in this analysis (see Table 1) is comparable to the smallest of the catchments used by Szolgayova et al. (2014). Therefore, small catchments may not have sufficient water storage to influence the long-term dependence

5   in flow time series. Furthermore, an increase in imperviousness further limits the water storage capacity of the urban catchments; this may also contribute to the lack of apparent relationship between the H exponent and the catchment size.

Catchments wetness, as indicated by annual rainfall and specific mean streamflow, is also known to influence the Hurst exponent (Szolgayova et al., 2014). Generally, catchments with lower rainfall totals and lower specific mean

10   streamflow are found to have higher long-term dependence due to the longer dry weather periods and consequently longer low flow periods. In this study, weak but significant negative correlations were found between the H exponent and both annual rainfall ($\rho = -0.36$, $p < 0.05$) and specific mean streamflow ($\rho = -0.35$, $p < 0.05$), but only for the rescaled-range method, indicating that to some extent this holds true for smaller catchment sizes. However, as demonstrated above, catchment imperviousness seems to be the most influential parameter in

15   affecting long range correlations for these sites.

4 Conclusions

Catchment imperviousness has long been identified as a key environmental indicator for stream health (e.g., Arnold and Gibbons, 1996; Hatt et al., 2004). In this study, the percent imperviousness of urban catchments was

20   also related to the loss of long-term memory in the streamflow series as quantified by the Hurst exponent. Streamflow data series from catchments in the USA (Jovanovic et al., 2016) were combined with data from catchments in Australia (Hamel et al., 2015) to cover a large range of imperviousness, from catchments used for water supply in natural conditions to those that were heavily urbanized.

The Hurst exponent, calculated using both the rescaled-range statistics (a simpler method) and the more

25   sophisticated de-trended fluctuation analysis, decreased from values around 1 in natural catchments to values around 0.6 for highly urbanized catchments. The values of the Hurst exponent, which is now not listed in the large range of metrics often calculated to characterise river regimes (e.g., Poff et al., 2010; Hamel et al., 2015), were conducive to the classification of the catchments as natural, peri-urban, and urban. That is, the Hurst exponent showed fairly visible breakpoints between these catchment types and has been shown here to be an effective and

30   easy-to-estimate metric to distinguish different levels of catchment urbanization. The range of imperviousness associated with this classification scheme is comparable to ranges developed via other metrics in literature, but was obtained herein using a metric easily calculated from daily streamflow data that is routinely collected by water agencies. There are obvious benefits to such a method, which can be applied without the need to use expensive and time consuming water quality and biological measurements. A downside of the method is that the

35   estimation of the H exponent requires long time series (at least between 15 to 20 years); the method is thus not usable to determine the benefit of restoration activities on the short term.

Hydrology and
Earth System
Sciences
Discussions

Open Access
EGU

References

10 Arnold, C. L., Jr. & Gibbons, C. J. 1996. Impervious Surface Coverage: The Emergence of a Key Environmental Indicator. *Journal of the American Planning Association,* 62**,** 243-258.

Ausloos, M., Cerqueti, R. & Lupi, C. 2017. Long-range properties and data validity for hydrogeological time series: The case of the Paglia river. *Physica a-Statistical Mechanics and Its Applications,* 470**,** 39-50.

Beran, J. 1994. *Statistics for long-memory processes,* New York, Chapman and Hall.

15 Burns, M. J., Fletcher, T. D., Walsh, C. J., Ladson, A. R. & Hatt, B. E. 2012. Hydrologic shortcomings of conventional urban stormwater management and opportunities for reform. *Landscape and Urban Planning,* 105**,** 230-240.

Debusk, K. M., Hunt, W. F. & Line, D. E. 2011. Bioretention Outflow: Does It Mimic Nonurban Watershed Shallow Interflow? *Journal of Hydrologic Engineering,* 16**,** 274-279.

Epps, T. H. & Hathaway, J. M. *in press.* Establishing a GIS Framework for the Spatial Identification of Effective Impervious
20   Areas in Gaged Basins: A Review and Case Study. *Journal of Sustainable Water in the Built Environment*.

Hamel, P., Daly, E. & Fletcher, T. D. 2013. Source-control stormwater management for mitigating the impacts of urbanisation on baseflow: A review. *Journal of Hydrology,* 485**,** 201-211.

Hamel, P., Daly, E. & Fletcher, T. D. 2015. Which baseflow metrics should be used in assessing flow regimes of urban streams? *Hydrological Processes,* 29**,** 4367-4378.

25 Hatt, B. E., Fletcher, T. D., Walsh, C. J. & Taylor, S. L. 2004. The influence of urban density and drainage infrastructure on the concentrations and loads of pollutants in small streams. *Environmental Management,* 34**,** 112-124.

Hirpa, F. A., Gebremichael, M. & Over, T. M. 2010. River flow fluctuation analysis: Effect of watershed area. *Water Resources Research,* 46.

Hurst, H. E. 1951. Long-term storage capacity of reservoirs.

30 Jovanovic, T., Mejia, A., Gall, H. & Gironas, J. 2016. Effect of urbanization on the long-term persistence of streamflow records. *Physica a-Statistical Mechanics and Its Applications,* 447**,** 208-221.

Kantelhardt, J. W., Koscielny-Bunde, E., Rybski, D., Braun, P., Bunde, A. & Havlin, S. 2006. Long-term persistence and multifractality of precipitation and river runoff records. *Journal of Geophysical Research: Atmospheres,* 111**,** n/a-n/a.

35 Kantelhardt, J. W., Zschiegner, S. A., Koscielny-Bunde, E., Havlin, S., Bunde, A. & Stanley, H. E. 2002. Multifractal detrended fluctuation analysis of nonstationary time series. *Physica A: Statistical Mechanics and its Applications,* 316**,** 87-114.

Kim, D. H., Rao, P. S. C., Kim, D. & Park, J. 2016. 1/f noise analyses of urbanization effects on streamflow characteristics. *Hydrological Processes,* 30**,** 1651-1664.

40 Koutsoyiannis, D. 2002. The Hurst phenomenon and fractional Gaussian noise made easy. *Hydrological Sciences Journal,* 47**,** 573-595.

Leopold, L. B. 1968. Hydrology for urban land planning - A guidebook on the hydrologic effects of urban land use. *Circular.* Reston, VA.

Li, Z. & Zhang, Y. K. 2007. Quantifying fractal dynamics of groundwater systems with detrended fluctuation analysis. *Journal*
45   *of Hydrology,* 336**,** 139-146.

Mandelbrot, B. B. & Wallis, J. R. 1969. Robustness of the rescaled range R/S in the measurement of noncyclic long run statistical dependence. *Water Resources Research,* 5**,** 967-988.

McDonnell, J. J. & Woods, R. 2004. On the need for catchment classification. *Journal of Hydrology,* 299**,** 2-3.

Mejía, A., Daly, E., Rossel, F., Jovanovic, T. & Gironás, J. 2014. A stochastic model of streamflow for urbanized basins.
50   *Water Resources Research,* 50**,** 1984-2001.

Montanari, A., Rosso, R. & Taqqu, M. S. 1997. Fractionally differenced ARIMA models applied to hydrologic time series: Identification, estimation, and simulation. *Water Resources Research,* 33**,** 1035-1044.

Mudelsee, M. 2007. Long memory of rivers from spatial aggregation. *Water Resources Research,* 43.

Olden, J. D. & Poff, N. L. 2003. Redundancy and the choice of hydrologic indices for characterizing streamflow regimes.
55   *River Research and Applications,* 19**,** 101-121.

Paul, M. J. & Meyer, J. L. 2001. Streams in the urban landscape. *Annual Review of Ecology and Systematics,* 32**,** 333-365.

Poff, N. L. 1997. Landscape filters and species traits: Towards mechanistic understanding and prediction in stream ecology. *Journal of the North American Benthological Society,* 16**,** 391-409.

Poff, N. L., Richter, B. D., Arthington, A. H., Bunn, S. E., Naiman, R. J., Kendy, E., Acreman, M., Apse, C., Bledsoe, B. P., Freeman, M. C., Henriksen, J., Jacobson, R. B., Kennen, J. G., Merritt, D. M., O'keeffe, J. H., Olden, J. D., Rogers, K., Tharme, R. E. & Warner, A. 2010. The ecological limits of hydrologic alteration (ELOHA): a new framework for developing regional environmental flow standards. *Freshwater Biology,* 55**,** 147-170.

Serinaldi, F. 2010. Use and misuse of some Hurst parameter estimators applied to stationary and non-stationary financial time series. *Physica A: Statistical Mechanics and its Applications,* 389**,** 2770-2781.

Sivakumar, B. & Singh, V. P. 2012. Hydrologic system complexity and nonlinear dynamic concepts for a catchment classification framework. *Hydrology and Earth System Sciences,* 16**,** 4119-4131.

Szolgayova, E., Laaha, G., Blöschl, G. & Bucher, C. 2014. Factors influencing long range dependence in streamflow of European rivers. *Hydrological Processes,* 28**,** 1573-1586.

Wagener, T., Sivapalan, M., Troch, P. & Woods, R. 2007. Catchment Classification and Hydrologic Similarity. *Geography Compass,* 1**,** 901-931.

Walsh, C. J., Fletcher, T. D. & Ladson, A. R. 2005a. Stream restoration in urban catchments through redesigning stormwater systems: looking to the catchment to save the stream. *Journal of the North American Benthological Society,* 24**,** 690-705.

Walsh, C. J., Roy, A. H., Feminella, J. W., Cottingham, P. D., Groffman, P. M. & Morgan, R. P. 2005b. The urban stream syndrome: current knowledge and the search for a cure. *Journal of the North American Benthological Society,* 24**,** 706-723.

Weron, R. 2002. Estimating long-range dependence: Finite sample properties and confidence intervals. *Physica A: Statistical Mechanics and its Applications,* 312**,** 285-299.
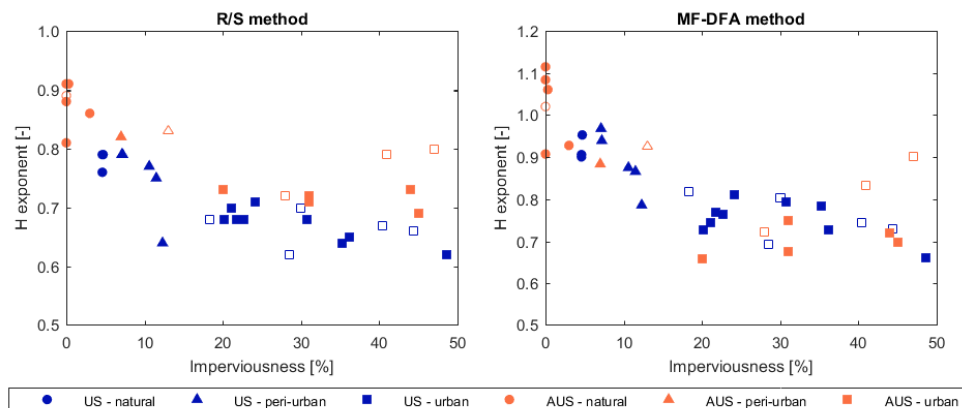
Figure 1. Relationship between the percentage of catchment impervious area and the H exponent estimated with R/S method (left) and with MF-DFA method (right) for catchments in the USA and Australia. Time series with gaps longer than 200 consecutive days have empty markers.
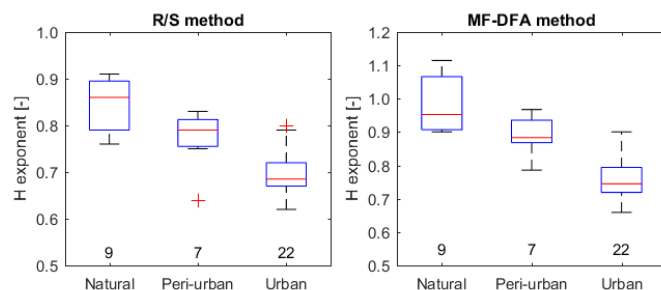
5

Figure 2. Empirical probability distributions of the H-exponent estimated with R/S method (left) and with MF-DFA method (right) grouped into natural (U<5%), peri-urban (U=5-15%) and urban (U >15%) catchments in the USA and Australia. Numbers below
10 the boxplots indicate number of data points used to generate the empirical distributions.
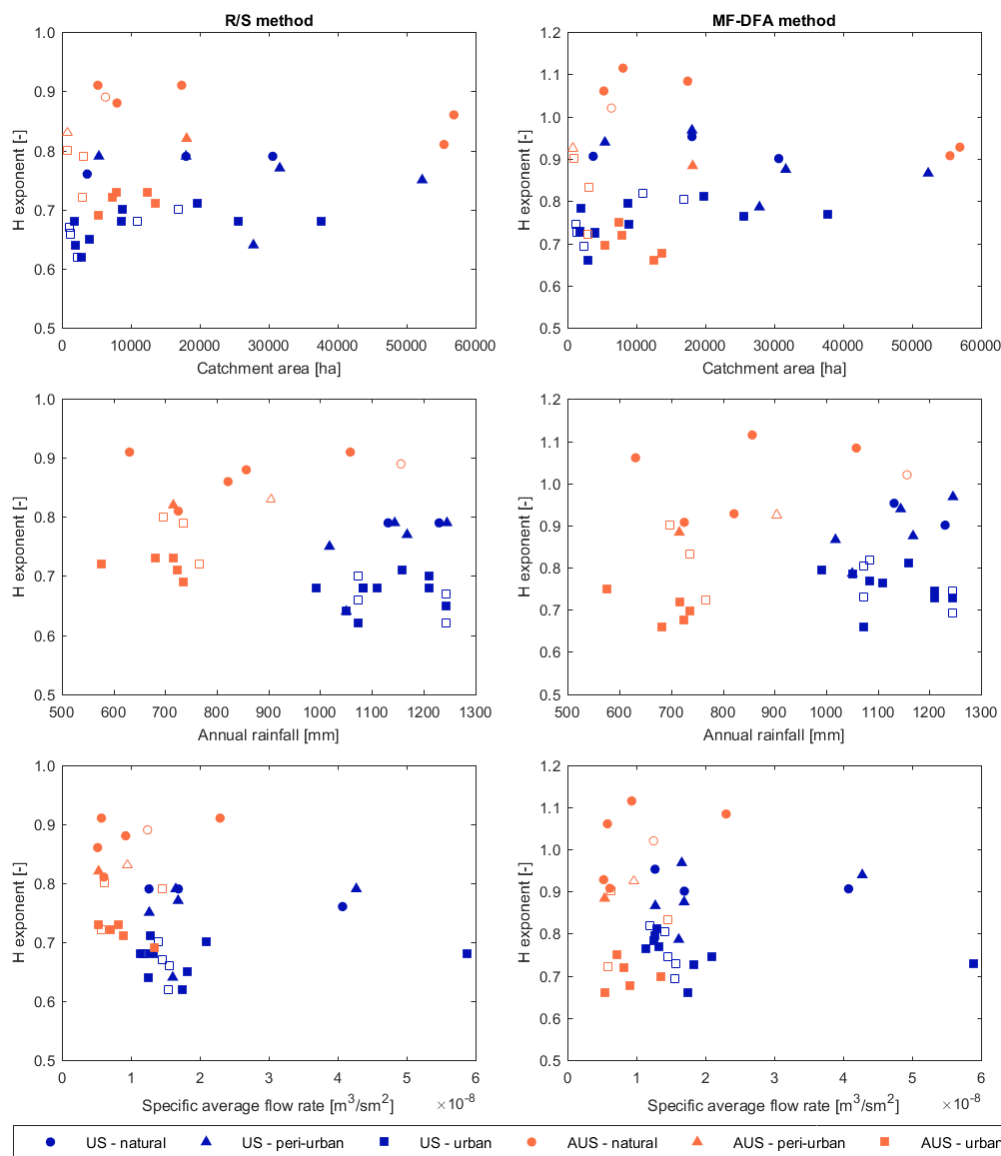
Figure 3. Relationship between the Hurst exponent (estimated with R/S method (left) and with MF-DFA method (right)) and the catchment size (top), annual rainfall (middle) and average flow rate per unit area (bottom) for catchments in the USA and Australia. Time series with gaps longer than 200 consecutive days have empty markers.

Table 1. US and Australian streamflow monitoring stations with monitoring period, number of missing days, fraction of impervious area, and total catchment area. Grey cells indicate monitoring stations with a gaps in time series longer than 200 consecutive days.

No.	Name	Gauge ID	Location	From – To (number of years)	Total missing days (consecutive missing days)	Impervious fraction U [%]	Catchment Area [ha]
1	French Creek	1472157	US	1968-2013 (45)	/	4.6	15310
2	Hunting Creek	1641000	US	1949-1992 (43)	/	4.6	1840
3	Patuxent River	1591000	US	1944-2013 (69)	/	4.7	9010
4	Winters Run	1581700	US	1967-2013 (46)	/	7.1	9010
5	Raccoon Creek	1477120	US	1966-2014 (48)	/	7.2	2690
6	Chester Creek	1477000	US	1931-2013 (81)	/	10.6	15820
7	Seneca Creek	1645000	US	1930-2013 (83)	/	11.5	26160
8	Skippack Creek	1473120	US	1966-1994 (28)	/	12.3	13910
9	Northwest Branch Anacostia River (upper)	1650500	US	1923-2013 (90)	422 (330)	18.3	5460
10	South Branch Pennsauken Creek	1467081	US	1967-2014 (47)	203 (159)	20.2	900
11	Cooper River	1467150	US	1963-2013 (50)	/	21.1	4400
12	Northeast Branch Anacostia River	1649500	US	1938-2013 (75)	/	21.7	18860
13	Northwest Branch Anacostia River	1651000	US	1938-2013 (54)	/	22.7	12790
14	Little Patuxent River	1593500	US	1932-2013 (81)	/	24.2	9840
15	Stemmers Run	1585300	US	1958-1989 (31)	365 (365)	28.5	1160
16	Gwynns Falls	1589300	US	1957-2013 (56)	364 (273)	30.0	8420
17	Henson Creek	1653500	US	1948-1978 (65)	/	30.8	4330
18	Watts Branch	1645200	US	1957-1987 (30)	/	35.3	960
19	Whitemarsh Run	1585100	US	1959-2013 (54)	158 (92)	36.2	1970
20	West Branch Herring Run	1585200	US	1957-2013 (56)	579 (273)	40.4	550
21	East Branch Herbert Run	1589100	US	1957-2013 (56)	365 (273)	44.4	640
22	Dead Run	1589330	US	1959-2013 (54)	282 (189)	48.6	1430
23	Lang Lang River	228209B	AUS	1985 - 2011 (27)	9 (2)	0.0	27743
24	McMahons Creek	229106A	AUS	1991 - 2008 (18)	767 (128)	0.0	4000
25	OShannassy River	229652A	AUS	1979 – 2008 (30)	1147 (196)	0.0	8700
26	Starvation Creek	229109A	AUS	1981 – 2008 (28)	2071 (972)	0.0	3160
27	Olinda Creek	229690	AUS	1992 - 2008 (17)	302 (102)	0.3	2610
28	Woori Yallock Creek	229679B	AUS	2000 – 2011 (12)	141 (31)	3.0	28460
29	Cardinia Creek	228228A	AUS	1985 - 2011 (27)	262 (105)	7.0	9060
30	Bungalook Creek	228369A	AUS	1985 - 2011 (27)	634 (236)	13.0	385
31	Cohranwarrabul Creek	228393A	AUS	1999 – 2011 (13)	50 (24)	20.0	6232
32	Brushy Creek	229249A	AUS	1992 - 2008 (17)	361 (281)	28.0	1470
33	Dandenong Creek @ Wantirna	228357A	AUS	1985 - 2011 (27)	173 (94)	31.0	6817
34	Mullum Creek	229648A	AUS	1992 - 2008 (17)	66 (13)	31.0	3700
35	Blind Creek @ Knox	228366A	AUS	1985 - 2011 (27)	483 (281)	41.0	1554
36	Gardiners Creek @ Ashwood	229625A	AUS	1992 - 2008 (17)	181 (72)	44.0	3950
37	Blind Creek @ High St	228351A	AUS	1985 - 2009 (25)	758 (185)	45.0	2656
38	Gardiners Creek @ Kinkora	229636A	AUS	1985 - 2011 (27)	1966 (213)	47.0	432